^{8}B structure in Fermionic Molecular Dynamics

KR Henninger, T Neff, H Feldmeier

GSI Helmholtzzentrum für Schwerionenforschung GmbH, Planckstrasse 1, 64291 Darmstadt, Germany

E-mail: k.henninger@gsi.de

Abstract. The structure of the light exotic nucleus ^{8}B is investigated in the Fermionic Molecular Dynamics (FMD) model. The decay of ^{8}B is responsible for almost the entire high-energy solar-neutrino flux, making structure calculations of ^{8}B important for determining the solar core temperature. ^{8}B is a proton halo candidate thought to exhibit clustering. FMD uses a wave-packet basis and is well-suited for modelling clustering and halos. For a multiconfiguration treatment we construct the many-body Hilbert space from antisymmetrised angular-momentum projected 8-particle states. First results show formation of a proton halo.

Introduction

The physics of weakly-bound nuclear systems is a fruitful area of study, which investigates the location of the proton- and neutron-driplines, as well as the structures occuring at such "exotic" proton-to-neutron ratios, such as the formation of neutron- and proton-halos. While there are several well-known neutron-halo nuclei, there are very few proton-halo candidates: the first excited state of ^{17}F, and the ground state of ^{8}B are the best-known.

The nucleus ^{8}B also plays a role in astrophysics, occuring in the third branch of the proton:proton (pp) chain. In fact, the decay of ^{8}B to ^{8}Be is responsible for over 75% of the high-energy solar neutrino flux [1]. Since this decay rate depends on the rate of production of ^{8}B via ^{7}Be(p,γ)^{8}B, (which is itself dependent on ^{8}B structure), knowledge of the ^{8}B ground state wavefunction is important input into such reaction calculations.

A proton halo in ^{8}B is inferred from the low proton binding energy of 0.137 MeV [2], narrow longitudinal momentum distribution of ^{7}Be following breakup [3] and a matter radius of 2.38 ± 0.04 fm [4], but ^{8}B proton radius is not known. An ^{8}B proton halo would affect the capture cross-section for a proton on ^{7}Be quite strongly, since the radiative capture process is dominated by contributions from regions far outside the nuclear radius [5].

^{7}Be is in itself loosely-bound [6], which means that the ^{8}B core may have the structure $\alpha + {}^3$He. What then, is the correct picture for ^{8}B? A shell-model type picture, a ^{7}Be core plus proton, or even the cluster structure $\alpha + {}^3\text{He} + \text{p}$? In order to access all these possibilities, one may choose to do such calculations in the Fermionic Molecular Dynamics (FMD) model, since it offers the possibility to access both shell-model type states and clustering (see [7] and refs. therein). FMD has been used for such diverse structures as the Hoyle state [8] and the neutron halo of ^{10}Be [9]. In this paper, I outline the model and present preliminary results for ^{8}B.

Fermionic Molecular Dynamics

Fermionic Molecular Dynamics (FMD) [10] is a microscopic model for light- to medium-mass nuclei. Overviews of the model are in [7, 10–12] and a summary is provided here.

Protons and neutrons are the relevant degrees of freedom in nuclear systems, so we choose intrinsic many-body configurations $|Q\rangle$, which are Slater determinants of single-particle states $|q\rangle$, or [10]:

$$|Q\rangle = \hat{\mathcal{A}}\{|q_1\rangle \otimes ... \otimes |q_A\rangle\} \tag{1}$$

where $\hat{\mathcal{A}}$ is the antisymmetrisation operator. The single-particle states are:

$$|q\rangle = \sum_i |a_i, \vec{b}_i\rangle \otimes |\chi_i^\uparrow, \chi_i^\downarrow\rangle \otimes |\xi_i\rangle c_i, \tag{2}$$

where a superposition of wave-packets $|a_i, \vec{b}_i\rangle$ can be used to describe extended distributions (*e.g.* halos). Parameters $\vec{b}$ relate to the mean position and mean momentum of the wave-packets and parameters a give the width of the wave-packets [11]. The ket $|\chi^\uparrow, \chi^\downarrow\rangle$ is the most general spinor, allowing all possible orientations of the nucleon spin. The isospin part of the state is given as $|\xi\rangle$ (*i.e.* proton or neutron).

In co-ordinate space one has:

$$\langle \vec{x}|a, \vec{b}\rangle = \exp\left\{-\frac{(\vec{x} - \vec{b})^2}{2a}\right\}. \tag{3}$$

Slater determinants like that in Equation 1 are not states of good angular momentum or parity, so these need to be projected out. The projection operators are given by [11]:

$$\begin{aligned} \hat{P}^\pi &= \frac{1}{2}(1 + \pi\hat{\Pi}) \\ \hat{P}^J_{MK} &= \frac{2J+1}{8\pi^2} \int d\Omega \, D^J_{MK}(\Omega)^* \hat{R}(\Omega), \end{aligned}$$

$$\tag{4}$$

where $D^J_{MK}(\alpha, \beta, \gamma)$ is the Wigner D-matrix, $\hat{R}(\alpha, \beta, \gamma)$ is the rotation operator and $\hat{\Pi}$ is the parity operator [7]. The action of the projection operators is to project states $|Q; J^\pi MK\rangle$ from intrinsic states $|Q\rangle$. There are potentially $2J + 1$ different K states for every state of good J, depending on the symmetries of the intrinsic state. By diagonalising the Hamiltonian in the set of K-projected states, we obtain the basis states

$$|Q; J^\pi M\alpha\rangle = \sum_K |Q; J^\pi MK\rangle c_K^{J^\pi \alpha}. \tag{5}$$

The parameters $\{q_\nu\}$ describing the intrinsic basis states $|Q\rangle$ are obtained by requiring:

$$\min_{\{q_\nu\}} \quad \frac{\langle Q; J^\pi M\alpha|\hat{H} - \hat{T}_{cm}|Q; J^\pi M\alpha\rangle}{\langle Q; J^\pi M\alpha|Q; J^\pi M\alpha\rangle}, \tag{6}$$

where $\hat{T}_{cm}$ is the operator for the centre-of-mass kinetic energy. The minimisation of the energy of the projected state (Equation 6) is referred to as Variation after Projection (VAP).

The VAP states $|Q; J^\pi M\alpha\rangle$ provide a good first approximation for the description of the nucleus. To improve the description, additional basis states can be generated by performing minimisation (Eq. 6) subject to constraints. These constraints could be on *e.g.* radii, moments or deformation parameters [7]. The FMD basis is general-enough to describe both shell-model like many-body states as well as clustering states [7].

^{8}B

Projected configurations with angular momenta and parities of 0+, 1+, 2+ and 3+ were created for ^{8}B, since with a ^{7}Be core (in its 3/2- ground state or first excited 1/2- state) plus a p3/2 proton, one can form states of total angular momentum 0 to 3. As per Equation 2, one Gaussian wave-packet was used to describe each of the neutrons and four of the protons in phase-space, while the fifth proton was described spatially by a superposition of two Gaussians, to allow for a possible extended distribution. A UCOM-transformed AV18 interaction [13] was used, for two reasons. Firstly, because AV18 is a realistic interaction (it reproduces the Nijmegen phase-shifts [14]), and secondly because, for application in FMD, the interaction is required to be in an operator representation, making UCOM the appropriate method to soften the interaction [13]. The Hamiltonian was diagonalised in this space, and ground- and excited state energies, radii and transition probabilities were extracted for the resulting eigenstates. Plots of the proton- and neutron-density distributions for the intrinsic states obtained by the VAP procedure are shown in Figure 1. One can note in this figure the appearance of clustering and of an extended distribution for a proton.

The level-scheme is provided as Fig 2. The calculated levels represent the energies for the eigenstates of the UCOM Hamiltonian, calculated in the space of VAP states. The calculated energies are compared to the calculated ^{7}Be threshold (the ground-state energy for ^{7}Be calculated in an FMD calculation); and one can note a slight underbinding with respect to threshold. Including more basis states (which will access more configurations) will improve this binding. The discrepancy between the experimental and theoretical binding energies is mainly due to missing tensor correlations in the FMD wave functions.

The radii and transition-strengths are provided in Tables 1 and 2 respectively. When considering the radii, one may note that the calculated matter radius is smaller than the measured radius. This is again due to the small basis set used: by including more basis configurations one may better-approximate the long tail for the spatial distribution of the loosely-bound proton and so improve the radius. One may note in Table 2 that the 3+→2+ transition is well-reproduced.

Table 1: Calculated rms matter-, charge-, proton- and neutron-radii, magnetic dipole moment (μ) and electric quadrupole moment (Q) for ^{8}B, for the basis of 4 VAP states (VAP). The calculations are compared to experiment, where values are known.

	R_{matter} [fm]	R_{charge} [fm]	R_p [fm]	R_n [fm]	μ [μ_N]	Q [efm^2]
Exp.	2.38±0.04 [4]				1.0355±0.0003 [15]	6.83±0.21 [16]
VAP	2.262	2.523	2.374	2.062	1.228	4.863

Table 2: Transition strengths $B(\Lambda M)$ calculated for the known transitions in ^{8}B (shown in black) and for some as-yet-unmeasured transitions (shown in red). Calculations were in the VAP basis as were those in Table 1. Where the character of the transition is not known, all possibilities are considered.

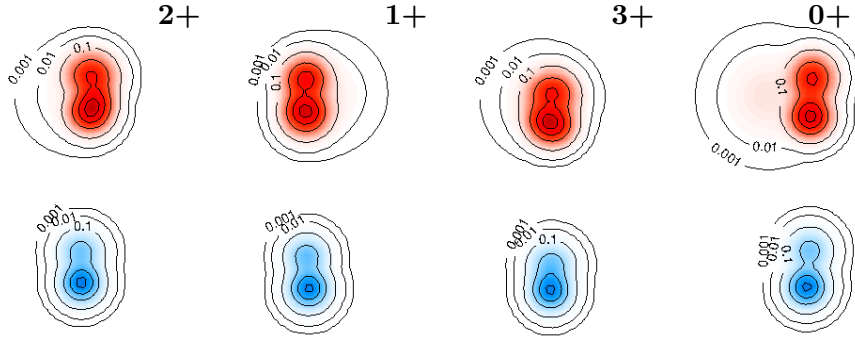| Energy [MeV]	States	Type	Basis	$B(\Lambda M)$ (meas.)	$B(\Lambda M)$ (calc.)
0.77	$1+ \to 2+$	$M1$	VAP	2.63(12) μ_N^2 [2]	3.992 μ_N^2
2.32	$3+ \to 2+$	$M1$	VAP	0.38(19) μ_N^2 [2]	0.274 μ_N^2
2.55	$2+ \to 2+$	$(M1)$	VAP		0.060 μ_N^2
3.30	$1+ \to 2+$	$(E2)$	VAP		5.438 e^2fm^4
	$1+ \to 2+$	$(M1)$	VAP		0.467 μ_N^2

Figure 1: Proton- (red) and neutron-densities (blue) for the VAP basis configurations. The numbers on the contour lines give nucleon density in units of the saturation density $\rho_0 = 0.17$fm^{-1}. Numbers to the right show angular momentum and parity of the configuration.
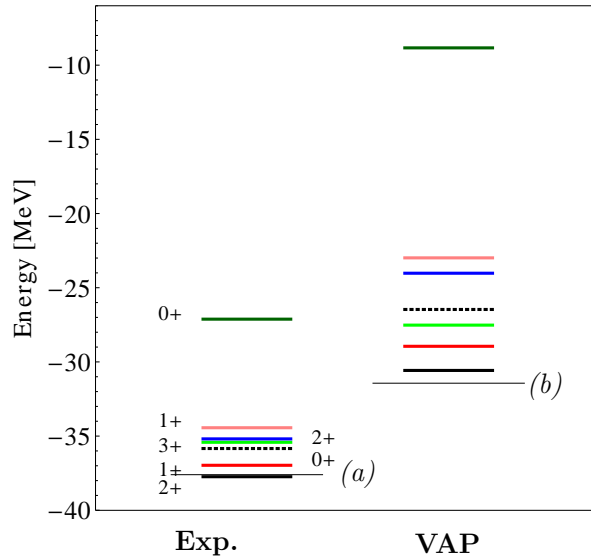
Figure 2: Level-scheme of ^{8}B comparing experimental and calculated ground and excited state energies. The thin lines indicate the ^{7}Be+p threshold in (*a*) the experimental and (*b*) the calculated case.

Conclusion

The large charge-, proton- and matter radii compared to neutron radius (Table 1) indicate proton halo formation in this model of ^{8}B. This is in line with previous studies (*e.g.* [3, 16, 17]). The extended proton distribution also shows up clearly in calculated proton densities (Fig. 1). Since all parameter values describing the nucleon states are dictated by the minimisation process (Eq. 6), including a second Gaussian wavepacket for the fifth proton *allows*, rather than *dictates*, its extended spatial distribution. If the second Gaussian were not needed to describe the proton's spatial distribution, its parameters would evaluate under minimisation such that its contribution would be negligible. Thus we may say that, under the interaction used, proton halo formation is indeed favoured in ^{8}B. Work on extending the basis by imposing constraints on matter-, proton- and neutron radii is underway.

References

[1] Xu H M *et al.* 1994. *Phys. Rev. Lett.*, **73**:2027.

[2] Tilley D R *et al.* 2004. *Nucl. Phys.* , **A745**:155.

[3] Smedberg M *et al.* 1999. *Phys. Lett.* B, **452**:1.

[4] Ozawa A *et al.* 2001. *Nucl. Phys.*, **A693**:32.

[5] Rolfs C S 1973. *Nucl. Phys.*, **A217**:27.

[6] Neff T 2011. *Phys. Rev. Lett.*, **106**:042502.

[7] Neff T and Feldmeier H 2010. *Cluster Structure in the FMD Approach*. (Research Signpost Publishing: Kerala). pp 67-94.

[8] Feldmeier H *et al.* 2007. *Phys. Rev. Lett.*, **98**:032501.

[9] Zakova A *et al.* 2010. *J. Phys.* G.: *Part. Nucl. Phys.*, **37**:055107.

[10] Feldmeier H and Schnack J 1997. *Prog. Part. Nucl. Phys.*, **39**:343.

[11] Neff T and Feldmeier H 2008. *Eur. Phys. J.* Special Topics, **156**:69.

[12] Bieler K Feldmeier H and Schnack J 1995. *Nucl. Phys.*, **A593**:493.

[13] Feldmeier H *et al.* 2005. *Phys. Rev.* C, **72**:034002.

[14] Wiringa R B Stoks V G J and Schiavilla R 1995. *Phys. Rev.* C, **51**:38.

[15] Shirley V S *et al.* (Eds.) 1996. *Table of Isotopes (Vol. 1)*. (John Wiley and sons publishing: New York).

[16] Minamisono T *et al.* 1992. *Phys. Rev. Lett.*, **69**:2058.

[17] Werner R E *et al.* 1995. *Phys. Rev.* C, **52**:1106(R).